

Northwest Atlantic



Fisheries Organization

Serial No. N512

NAFO SCR Doc. 82/VI/24

SCIENTIFIC COUNCIL MEETING - JUNE 1982

Physical Oceanographic Features and Processes Relevant to *Illex illecebrosus*
Spawning Areas and Subsequent Larval Distribution

by

R. W. Trites

Marine Ecology Laboratory, Bedford Institute of Oceanography
P. O. Box 1006, Dartmouth, Nova Scotia, Canada B2Y 4A2

Introduction

The Working Group on Squid Research within NAFO identified 5 scenarios concerning where short finned squid (*Illex illecebrosus*) may spawn and subsequently how the juveniles return to the continental shelves of the Canadian Atlantic Seaboard (Anon, 1981). This paper will address principally one of these scenarios. Following assumptions of suitable environmental conditions for spawning will be made, a larval dispersion model is developed to predict an idealized larval distribution over a period of about 1-2 months following spawning.

The laboratory work of O'Dor *et al.* (1981) indicated that the eggs of *I. illecebrosus* do not develop at temperatures below 13°C. The only egg mass in which normal development was seen, was spawned at 13°C and developed at an average temperature of 14°C to produce normal hatchlings after 11 days. Boletzki *et al.* (1973) reported that *I. coindetii* develop normally at 15°C but fail at 10°C. O'Dor *et al.* (1981) found that the egg mass was deposited on the bottom of the tank and expressed the view that under oceanic conditions freely floating eggs would be unlikely to hatch successfully. This paper will be developed, therefore, on the assumption that squid spawn only on bottom and where temperatures exceed 13°C.

Seasonal Thermal Structure and Bottom Temperatures

The waters of the continental shelf between Cape Hatteras and the Grand Banks undergo a pronounced seasonal cycle of heating and cooling. This seasonal cycle is most pronounced at the sea surface and becomes progressively damped with depth, and in general is confined to the upper 100-200 m of the water column.

Generally speaking, there is a phase lag with depth in the timing of the seasonal maximum and minimum temperatures.

For the inshore area between the Gulf of Maine and Cape Hatteras, daily temperature profiles have been taken at a number of lightship sites for a number of years. Data from a several of these sites (Fig. 1) have been examined for the period 1956-60. To illustrate the general nature of the seasonal cycle, one year's data for Portland, Chesapeake, and Diamond Shoals Lightships are plotted in Figures 2, 3, and 4, respectively. Data for the 7 sites depicted in Figure 1 were examined for the 5-year period, and the time when the bottom temperature reached 13°C and again when it fell below 13°C was noted (Table 1). These measurements were taken on the shelf and over a range of depths from 17 to 55 m. Care must therefore be taken in inferring the overall representativeness of the measurements in any very detailed sense. Also the data show marked year to year variations. Nevertheless, apart from areas shallower than about 20 m, the maximum bottom temperatures under normal conditions, do not exceed 13°C on the continental shelf north of about 42°N at any time of the year.

At Nantucket Lightship, bottom temperatures generally exceed 13°C for only about a 2 month period (late Sept. - late Nov). Further south, the period with above 13°C temperature increases until one reaches Cape Hatteras where the bottom temperature at Diamond Shoals rarely falls below 13°C.

Bigelow (1932) in his studies on the waters of the continental shelf between Cape Cod and Cape Hatteras, presented a series of temperature sections across the shelf for different seasons of the year, and as well presented maps of bottom temperatures. Temperature sections south of Cape Cod and off Chesapeake Bay at the end of October 1931 and 1919, respectively (Fig. 5) show the general characteristics. Basically, the area of bottom temperatures >13°C is confined inshore and decreases towards the northeast. A plot of bottom temperature is shown in Figure 6 for the period 19-29 Oct., 1931.

Surface waters, along the continental shelf, typically reach maximum values during August. However, the maximum value at depth is normally reached at progressively later times at greater depths in the water column, and may occur several months later at, say 100 m.

Although the surface-layer waters over the continental shelf from the Grand Banks to Cape Hatteras is generally classed as "Coastal Water" or "Shelf Water", it is bounded on the seaward side by a water mass classed as "Slope Water".

A good schematic illustration of the general water mass structure for this part of the northwest Atlantic, taken from Islen (1936), is shown in Figure 7. The boundaries or fronts between these waters are convoluted and are regions of interacting water masses, strong temperature and salinity gradients and continual change. In the mid-Atlantic Bight the boundary between Coastal and Slope Water at the bottom is generally located near the shelf break close to the 100 m contour (Wright, 1976) and slopes upward offshore, intersecting the surface roughly 50 km further seaward. Thus the seasonal pattern of bottom temperatures in the shelf-slope area is markedly different from that of the inner continental shelf area. The net affect of this Slope Water is to produce maximum bottom temperatures along the shelf break in the Autumn winter period. Bottom temperature data reported in Bigelow (1933) for the 19-21 Dec., 1932, show Slope Water present along the shelf break near the 100 m contour (Fig. 8).

Northern Spawning Area Limits

For Illex illecebrosus, assuming spawning on bottom and at temperatures $> 13^{\circ}\text{C}$, the picture emerges that in terms of suitable physical conditions the northern limits of spawning, would be in the Cape Cod-Georges Bank region. The continental shelf from Cape Hatteras southward is suitable the year round in terms of meeting the minimum temperature criteria. As one progresses northward from Cape Hatteras the period, for the inner continental shelf areas, diminishes to about 6 months off Chesapeake Bay, 3 months off New York, 2 months at Nantucket, and zero within the Gulf of Maine and northward. In the October-November period the limits of $>13^{\circ}$ inshore, shelf bottom water recedes rapidly southward towards Cape Hatteras (Fig. 9). The shelf break area, however, behaves differently from the inshore area, being in the Shelf Water/Slope Water boundary zone. Wright (1976) studied the thermal features of the shelf-slope area between $69-72^{\circ}\text{W}$, using 32 years of data, and showed that the Shelf Water/Slope Water boundary, identified by the 10°C isotherm, intersects the bottom within 16 km of the 100 m isobath about 80% of the time. Maximum temperature of the Slope Water on the bottom showed a seasonal variation of about 2°C , with an annual mean of 13.2°C . Above 13°C maximum-temperature water was present in the August-February period, with the annual maximum occurring in December. Although Wright's studies do not show statistical limits for the areal extent of $>13^{\circ}\text{C}$ bottom water, examination of Bigelow's data (1933), and others, indicates

that it is unlikely to reach much deeper than about the 200 m isobath. In Fig. 9 it has been assumed that water $>13^{\circ}\text{C}$, while normally present throughout the entire length of the shelf-slope area between Cape Hatteras and Cape Cod, is confined to the 100-200 m depth zone.

Lange and Sissenwine (1981) report that Illex illecebrosus, in the area off northeastern United States, probably spawn to some extent through most of the year, although autumn samples contained the highest proportions of mature individuals in most years. No spawning has been observed off the Nova Scotia or Newfoundland coasts, and this is consistent with the assumption that bottom temperatures are always sub-critical. The departure of adult squid from the Canadian continental shelf waters in early autumn is noteworthy. Of particular significance is the fact that squid can travel long distances in comparatively short times. Dawe et al. (1981) report the late-season recovery off the coast of Maryland of a short-finned squid tagged in Notre Dame Bay, Newfoundland. This migrant had travelled at least 1260 naut. mi. in 107 days (Fig. 10). Using the temperature criteria set forth previously, this squid may have already reached 13°C bottom water since it was recovered in the 100-200 m depth zone. On the other hand if it were to spawn in shallower waters, it would have had to continue on to nearly Cape Hatteras before encountering 13°C bottom water.

Juvenile squid ranging in length from 10-30 mm are observed in the February-March period in the Slope Water-Gulf Stream frontal zone (Fedulov and Froerman, 1980; Dawe et al., 1981). Although growth rates at the larval-juvenile stage are unknown, Squires (1967), concluded that Illex probably mature within the first year with an average 12-month growth rate of 2.8 cm/month, and an average of 4.7 cm/m over the first 3 months. Thus, on this basis, squid in the 10-30 mm length range are probably less than 2 months old. Based on this assumption, and as well that Illex spawn on bottom in water $>13^{\circ}\text{C}$, then it appears that spawning may peak in the December-January period, with highest probability in the area south of Chesapeake Bay and possibly even south of Cape Hatteras.

Chesapeake Bay-Cape Hatteras Area as an assumed spawning area.

If larvae are "released" from the bottom in the Chesapeake Bay-Cape Hatteras area, what dispersion pattern might one expect? Firstly, if one assumes they were neutrally buoyant and immobile, they would be expected to behave much like the surrounding water mass. At this time of year the water is virtually homogeneous from top to bottom (Figs. 3 and 4). Bumpus (1973) in his summary of

a 10-year program of drift-bottle and seabed drifter releases, concluded that a mean alongshore flow of about $5 \text{ cm}\cdot\text{s}^{-1}$ occurs from Cape Cod to Cape Hatteras. Beardsley et al. (1976) have determined the "mean" or residual current field from moored current meters in the mid-Atlantic Bight (Fig. 11). Only records of one month or longer duration have been used, and the mean currents are plotted as vectors with the magnitude equal to the average speed. The depth in meters of an individual measurement is indicated by a small number located near the head of the current vector. Winter measurements are denoted by solid vectors and summer ones with dashed vectors. From these it is noted that the flow near Section III is southerly at all depths and in both summer and winter for the three outermost stations, at speeds varying from $10\text{-}20 \text{ cm}\cdot\text{s}^{-1}$.

One would expect, therefore, that larvae under the foregoing conditions, would be mixed throughout the water column on the Shelf within a matter of hours. Advection southward would transport them to Cape Hatteras within a period of days. Since Cape Hatteras normally acts as a barrier to continued southward alongshore flow, the flow turns seaward and becomes entrained in the Gulf Stream (Beardsley et al. 1976).

Before addressing specifically the eastward transport in the Gulf Stream system, a theoretical review of particle diffusion and dispersion in shear flow will be given.

Diffusion and Dispersion Processes

The process of oceanic diffusion is complex and there is no single theory existing that can explain or interpret the entire pattern of diffusion. In practice, therefore, progress in understanding oceanic diffusion depends heavily on an empirical approach by means of tracer experiments.

If a substance (S) with a concentration of S_0 were continuously introduced at a position X_0 in water moving uniformly with a velocity U_0 in the x- direction, one typically would find that the substance spreads out into an ever broadening plume as the distance from the source increases. Maximum concentrations also decrease away from the source. This phenomenon is illustrated schematically in Figure 12. Typically the concentration distribution across the plume is Gaussian, and in practice one uses the variance, σ^2 , to describe the diffusion characteristics and the plume width as 4σ , which encompasses some 95% of the diffusing substance.

In addition to the diffusion of a substance through the turbulent or eddying water motion, its spread will be further enhanced if there are gradients (shear) in the mean flow field. Schematically the effect of horizontal velocity shear is illustrated in Figure 13. In the no-shear situation one would expect diffusion away from an instantaneous point source to be radially symmetric, with the limits of the patch size increasing with time. In the presence of horizontal shear, however, the substance will tend to become stretched out in the direction of flow since material diffusing into the area of higher velocity will be advected faster than the mean and slower than the mean for material diffusing into the lower velocity area.

The distributions of a conservative property, S, in the sea can be represented in terms of a differential equation.

$$\begin{aligned} \frac{\partial S}{\partial t} &= u \frac{\partial S}{\partial x} + v \frac{\partial S}{\partial y} + w \frac{\partial S}{\partial z} \\ &= \frac{\partial}{\partial x} \left(A_x \frac{\partial S}{\partial x} \right) + \frac{\partial}{\partial y} \left(A_y \frac{\partial S}{\partial y} \right) + \frac{\partial}{\partial z} \left(A_z \frac{\partial S}{\partial z} \right) \end{aligned} \quad (1)$$

where:

S = S(x, y, z, t) = concentration

x = eastward direction

y = northward direction

z = downward direction

t = time

u, v, w = velocity in x, y, z, direction respectively

A_x, A_y, A_z = Eddy diffusion coefficients

The eddy diffusion coefficients are considered to be analogous with molecular diffusion coefficients, but many orders of magnitude larger, because they incorporate the effect of turbulent mixing.

As no general solution to equation (1) has yet been found, some simplifying assumptions must be made, to enable a solution to be found.

Specifically, assume that diffusion is confined to the horizontal direction, is independent of position, that the water is homogeneous over a depth d, that the flow is only in the x-direction, and that the shear, Ω, is constant so U = U₀ - Ω y where U₀ = mean velocity. Equation (1) thus becomes

$$\frac{\partial S}{\partial t} + (U_0 - \Omega y) \frac{\partial S}{\partial x} = A_x \frac{\partial^2 S}{\partial x^2} + A_y \frac{\partial^2 S}{\partial y^2} \quad (2)$$

Since the mean velocity has nothing to do with the dispersion of S, (which for convenience we will refer to as concentration of squid larvae), we can eliminate U_0 from the equation, with the understanding that the coordinate system x, y, z in equation (2) is moving with the center of gravity of the patch of squid larvae.

Assuming a point source of larvae such that, as initial conditions ($t=0$), a mass Q of squid larvae are introduced into the water column at $x = y = 0$. Then, as shown by Carter and Okebo (1965), a solution of equation (2) is:

$$S(x,y,t) = \frac{Q}{4 (A_x A_y)^{1/2} t \left(1 + \frac{\Omega^2 A_y}{12 A_x} t^2\right)^{1/2}} \cdot \exp \beta \dots \quad (3)$$

$$\text{where } \beta = \frac{\frac{A_x}{A_y} \left(1 + \frac{\Omega^2 A_y}{3 A_x} t^2\right) y^2}{4 A_x t \left(1 + \frac{\Omega^2 A_y}{12 A_x} t^2\right)}$$

Equation (3) having a quadratic form in x and y , states that the contours of concentration are a set of ellipses with a common principal axes, whose orientation varies with time. Thus the larval squid patch is elongated in the direction of flow. The variance in the major principal axis grows as the cube of the time (t^3) and the square of the shear (Ω^2). After a sufficiently long time, the patch of larvae will line up in the direction of the mean flow.

On the basis of equation (3) one can compute a number of characteristics of the diffusion such as the peak concentration S_p , the variances, σ_x^2 and σ_y^2 and the stretching factor, ρ , (i.e. the ratio of the major to the minor axes of the ellipse).

Since we are only interested in very long diffusion times, i.e., days to weeks, the forms of these parameters can be simplified as shown in Table 2.

Dispersion From a Continuous Source

The foregoing model, while providing insight into the nature of dispersion from an instantaneous point source, is not realistically applicable to squid larval

dispersion, since spawning and hatching will occur over an interval of time. A model is needed that predicts subsequent distribution from a squid larval source that is continuous over a period of several weeks.

Okubo and Karweit (1969) dealt with the application of the shear-diffusion solution for a continuous release of a passive contaminant in a flow with uniform shear both laterally and vertically. Basically, the solution assumes that a plume may be assembled by the superposition of an infinite number of patches released from a fixed origin and translated by the mean flow. Figure 13 is a schematic representation of the individual patches, and the envelope surrounding them for both a uniform and a shear flow. Okubo and Karweit (1969), in their numerical solution, found that the cross-sectional distributions of concentration became skewed, at increasing distances from the source, to the side where the velocity is smaller (Fig. 14). They explain this effect in the following way: in general, the lateral spread at a given distance from the source is determined by the time that the flow needs to cover the distance. This time is longer at the site where the flow has lower velocities and shorter where the velocity is greater. Hence, the lateral spread will be wider at the site of the smaller mean velocity.

The concentration isopleths are illustrated schematically in Figure 15, and the locus of maximum concentration (y_m) is plotted as well. At long diffusion times, when the shear effect becomes relatively important in mixing, the maximum concentration is seen to bend in the direction where the mean velocity is greater. The overall rate of decrease in the peak concentration is nearly inversely proportional to the distance away from the source. Another interesting result is that, if the horizontal velocity is decreasing with depth, then maximum concentration is found at the sea surface.

While lines of constant concentration are of interest with respect to larval dispersion, it is of equal interest to know how the age-frequency distribution curves should vary geographically. While it is not proposed to develop an analytical model of the precise distribution, a semi-quantitative interpretation will be attempted. If larvae have been released into the water column for say, 100 time units, then at $t = 100$, the larvae which have reached the furthestmost downstream will be all age 100, but at exceedingly low concentrations. At the source the larvae will all be at age 0, and highly concentrated. To a first approximation the mode of the age-frequency distribution will shift smoothly from 0 to 100 along the axis of peak concentration. At any given cross-section, normal to the locus of peak

concentration, the age mode will be highest at the northern most point (where the velocities are lowest) and lowest at the southernmost point (where the velocities are highest). Under certain values of shear, and horizontal eddy diffusion, the isopleths of age mode might appear as in Fig. 16.

Flow Characteristics in Gulf Stream

Before evaluation of the various parameters identified in the previous sections, let us review briefly some of the important features in the Gulf Stream flow pattern.

Currents in the Gulf Stream have been measured or computed using a variety of techniques, such as observing ship drift (Loran), measuring surface currents with a geomagnetic-electro-kinetograph (G.E.K.), and by dynamic computations from temperature and salinity data. More recently satellite tracked drogues have provided accurate and frequent "fixing" of drifting buoys over many months.

In the Gulf Stream peak velocities of $200-250 \text{ cm}\cdot\text{s}^{-1}$ are commonly encountered. Worthington (1954) measured and computed velocities through 3 sections across the Stream in October-November, 1950, in the vicinity of $68-69^{\circ}\text{W}$. In Fig. 17 the surface velocities through each of these sections are shown, with the results from GEK, Loran, and dynamic computations plotted. The results of all 3 methods are in relatively good agreement and show that on average the horizontal shear is strongest near the northern edge of the stream. Shear in this part of the flow ranged from about 3×10^{-5} to $8 \times 10^{-5} \text{ s}^{-1}$ for a mean of about $6 \times 10^{-5} \text{ s}^{-1}$. Mean current through this shear zone was about $100 \text{ cm}\cdot\text{s}^{-1}$ and reached a mean maximum of about $200 \text{ cm}\cdot\text{s}^{-1}$.

Attention is drawn as well, to the geographic position of the zero crossing of the surface velocity in relation to the thermal structure. As a survey tool, one commonly uses the position where the 10°C isotherm is at 500 m (or the 15°C isotherm at 200 m) to delineate the high-velocity core of the Stream. Thus the position of these isotherms, at their respective depths, are in all three cases well south of the position of zero surface velocity. The northern edge of the Stream, on a water-mass basis may not be at the zero velocity position, since Slope Water and various admixtures of Slope Water-Coastal Water-Gulf Stream may also be moving in the direction of the Stream.

Geostrophic currents, assuming no motion at 2000 m, were computed by Worthington (1954) for the 3 sections and are shown in Fig. 18. Although these computations indicate that the Stream tends to be composed of a series of jets,

perhaps more importantly for our consideration here is the broad picture - i.e. the core of maximum current is confined to a depth of less than 200 m and in terms of velocities, currents of $>20 \text{ cm.s}^{-1}$ are confined to the upper 1000 m.

The advent of satellite tracking of drifting buoy technology has enabled new data on the kinematics of the Gulf Stream to be acquired. Kirwan *et al.* (1976), reported on the results of a buoy launched off Florida on 20 July 1975 and tracked for 6 months (Fig. 19). It was drogued with a parachute at the end of 35 m of wire. Of particular interest is the travel time from Cape Hatteras to about 55°W . Although the trajectory was wavelike, the transit was completed in about 15 days. A maximum drift speed in excess of 250 cm.s^{-1} was found for a short period, and it averaged well over 150 cm.s^{-1} for this 15-day period. The mean, straight-line transit velocity for the 15-day period was in excess of 140 cm.s^{-1} .

Other buoys deployed in the Northwest Atlantic for different purposes have become entrained in the Gulf Stream during part of their lifetime. Extracts from three of these are depicted in Fig. 20. For buoy 0252 which had a drogue at 200 M, it travelled from just off Cape Hatteras to 60°W in 14 days (Fig. 20A), for a mean strait-line velocity of about 120 cm.s^{-1} . Buoy 0512 (Fig. 20B) made a similar journey in 38 days. However of these 38 days it spent 24 days making three circuits of a Warm Core eddy before continuing eastward. The mean velocity when not in the eddy averaged about 120 cm.s^{-1} . Buoy 1301 (Fig. 20C) which was originally launched on Browns Bank, was caught in the Stream south of Georges Bank. Between 65° and 50° it averaged 50 cm.s^{-1} .

The general picture emerges that while the current speeds in the Stream tend to decrease towards the east, particularly eastward of 60°W , a mean speed between Cape Hatteras and 60°W , is typically in the range of $120\text{-}150 \text{ cm.s}^{-1}$.

Larval Dispersion Characteristics In Gulf Stream System

Based on the results of Worthington (1954) and the Satellite tracked buoys, a simple velocity structure will be assumed for the Gulf Stream as depicted in Fig. 21. It will be further assumed that the velocity profile remains unchanged between 75°W and 50°W , and that the Stream flows smoothly without meanders. The equation of particle dispersion in shear flow from an instantaneous point source, as developed in an earlier section, can be solved for a point source located off Cape Hatteras, and with realistic velocity and shear values.

In Table 3 patch characteristics are computed for two larval "injection" points. In the first example, it is assumed that the larvae are injected as an instantaneous pulse at the edge of the current where the velocity is zero.

Patch length in the direction of flow is given by:

$$2 [(\sigma_x)_t + (\sigma_y)_t]$$

For the injection at a point 12 km inside the shear zone the velocity at this point is 72 cm/sec and the larvae will remain entirely within the shear zone for 10 days. At this point, some larvae have reached the northern boundary where the current vanishes. At times longer than 10 days, the along-flow patch size is assumed to be given by:

$$2 [(\sigma_x)_t + (\sigma_x)_{10} - (\sigma_y)_{t-10}]$$

Plots of these patch locations assuming a simple Gulf Stream with a width of 100 km, are sketched in Figs. 22 and 23. Several points should be noted. Firstly, the shear is responsible for producing a tremendous stretching of the patch in a direction nearly parallel to the edge of the Gulf Stream. The patch length to width ratio after 30 days is about 50. Secondly, the patch length for Example 1 after 20 days extends from a point west of 75°W along the northern edge of the Stream, to approximately 60°W. For Example 2, the patch would extend to about 57°W, in the same length of time. Thirdly, the patch width, even after 30 days is only a little more than one-half the width of the Gulf Stream. In Example 1 the patch limits penetrate a comparable distance (normal to the flow) into the Gulf Stream and Slope Water (assuming the Gulf Stream is bounded by the zero velocity line). In Example 2 the proportions are approximately 71:29 respectively.

For a continuous point source of new larvae over a period of 30 days the larval distribution will be essentially contained within the envelope of a 30 day ensemble of patches, with, on theoretical grounds, a slight bending of the line of peak larval concentrations towards the zone of maximum velocity of the Stream. The shear produces major asymmetry in terms of the geographic variation in age-frequency distribution. The isopleths of the age-frequency mode will, in Example 2, cut across the Stream at a very small angle. Thus at any given time and for any given section across the stream the proportion of younger larvae should increase as one moves from the northern limit in Slope Water to the southern boundary in the

Stream. It should be noted in this idealized situation the larvae are all confined to a section that is relatively narrow, and at most is unlikely to exceed 60 km in width.

Role of Gulf Stream Eddies

The process of formation of Gulf Stream Eddies begins when the Stream starts to meander as it flows northeastward and away from the North American continent at Cape Hatteras. If the meander develops into a major loop it may detach from the Stream and become an eddy. The result is a ring of high-velocity Gulf Stream Water circulating clockwise around a core of water of different origin. Often the term Gulf Stream Ring is used to describe these eddies. An eddy that forms to the north of the stream will have a core of water from the Sargasso Sea, and is referred to as a warm-core eddy. Conversely, an eddy that forms to the south of the Gulf Stream will have a core of water drawn from north of the Stream (Slope Water), and hence colder. It is referred to as a cold core eddy and is rotating counter clockwise.

Eddies have a wide range of lifetimes from barely a week to possibly as long as three years. In the case of cold core eddies the average lifetime has been estimated as one to one and one-half years (Wiebe, 1982). A census of warm core rings reported by Mizenko *et al.*, 1978, Ceylone and Chamberlin, 1980, etc. indicates that for the region west of 60°W the number of eddies formed per year in the 1976-80 period varied from 5 to 8. Satellite imagery reveals that warm-core eddies form east of 60°W as well, but there is as yet little documentation on their numbers and duration. The warm core eddies formed west of 60°W, in general, move southwestward and may reach as far as Cape Hatteras before being reabsorbed into the Stream. Their average lifetimes are shorter than for cold core eddies, with most of them disappearing in the first year of life. For those formed east of 60°W, it appears that their lifetime is much less than their western neighbours.

Noting from the previous section that the larval dispersion pattern for releases at the edge of, or just within, the Gulf Stream off Cape Hatteras tend to be confined to the area near the north wall of the Gulf Stream, let us sketch a scenario for a sequence of small patches being carried by the Stream during the period a warm and cold core eddy are being created (Fig. 24). For this illustration shear is being ignored, and the center of the patch is considered to be moving with a velocity of about 120 cm.s⁻¹. The mean larval age in days is shown inside the

small circles. The scenario depicts the formation of both a warm-core and cold-core eddy at about 65°W over a 10 day period. The following points should be noted: larvae tend to be found on the exterior boundary of a warm-core eddy and in the central part of the cold core eddy; for the Gulf Stream the effect of the eddy formation is to produce a discontinuity in terms of age increase along the stream. With the lapse of time, the mean age of larvae in the eddies will be much older than the mean in the Gulf Stream at the same longitude.

A few additional comments about eddies, and their importance in larval transfer into Slope Water and the Sargasso Sea, are warranted. Noting that the larvae should in fact be stretched out along the entire length of the Stream in this area, and if the insertion rate is constant, then the number of larvae per unit length of the Gulf Stream-Slope Water boundary will be nearly uniform assuming that the Stream width remains constant. Since the larvae are located near the periphery of a warm-core eddy and along the interior ring of a cold-core eddy, there will be many more larvae, in total, in a warm-core eddy compared to a cold-core one. It appears likely that the numbers contained in a warm-core eddy would generally be at least an order of magnitude greater than those for a cold-core eddy.

If two warm core eddies with a diameter of 200 km were formed during a period larvae were concentrated along the northern edge of the Gulf Stream, then a 1200 km "length" of larvae would be transported into Slope Water by the eddies. This represents about 25% of the smooth Gulf Stream length between Cape Hatteras and the Tail of the Grand Banks.

Discussion

If it is assumed that spawning reaches a peak that is largely contained within a period of a few weeks, one needs to consider as well the larval distribution during the "decay" period, when the supply has diminished to near zero. At any given longitude one would expect larvae to disappear first from the high velocity part of the Gulf Stream and remain for the longest time in the low velocity areas north of the Gulf Stream.

The treatment of larval dispersion and concentration has assumed that larvae can be treated as a conservative scalar quantity and drift passively with the surrounding water. The role that mortality may play has been neglected. However, the effect could easily be included if one assumed that the fraction of

larvae lost, due to mortality was a constant k , then equation (1) would have an additional term, kS .

The solution (Equation 3) would be multiplied by e^{-kt} . If the mortality rate k , is sufficiently high it will have a major effect on the concentration levels. It will not however change the pattern of the dispersing patch.

The assumption that the larvae behave as inert, neutrally buoyant particles, is probably a reasonable one for recently hatched larvae in a highly turbulent regime. However, it eventually will become totally untenable at some later stage in their growth and development. Vertical movements of even a few tens of meters may produce important differences in distributional pattern owing to vertical variations in currents and turbulence. If one assumes that the sustained swimming speed (in $\text{mm}\cdot\text{s}^{-1}$) of squid is roughly equal to their length in mm, then a squid of say 10 mm could achieve a vertical migration of 1000 m in less than 3 hrs. When the juveniles reach a size where sustained swimming speeds of $5\text{-}10\text{ cm s}^{-1}$ are possible, then their horizontal distribution, outside of high velocity areas such as the Gulf Stream, is likely to be more dependent on their swimming activity than on the current patterns.

The models developed here are based on the assumption that recently hatched larvae are entrained into the northern edge of the Gulf Stream in the vicinity of Cape Hatteras and are rapidly advected northeastward and dispersed. Although a long strip of bottom between Cape Hatteras and Cape Cod, within the 100-200 m depth zone appears likely to have temperatures exceeding 13°C in the August-February period, and hence might be considered as a suitable spawning area, it appears that most of it can be ruled out as a larval source area for larvae subsequently found in the Gulf Stream-Slope Water area in the January-March period. The southwestward currents along the shelf and slope northeast of Chesapeake Bay are commonly less than $10\text{ cm}\cdot\text{s}^{-1}$, so that larvae released in this area would have become juveniles before reaching Cape Hatteras and the Gulf Stream. Thus, on the assumption that *Illex* spawn on bottom, in water above 13°C , and larvae subsequently found in the Gulf Stream, the only geographic area meeting these criteria is located south of Chesapeake Bay.

Using lateral diffusion coefficients, derived from a wide range of oceanic dye diffusion experiments, and a simple, unidirectional flow regime with linear shear indicates that larvae entering the shear zone of the Gulf Stream should, over a 30 day period, be distributed in a thin ribbon, some 3000 km long, and less than 60

km wide at its broadest point. The dynamic and kinematics of the Gulf Stream-Slope Water system is extremely complex and not, as yet, well understood. The meandering nature of the Stream, the creation and reabsorption of Gulf Stream eddies, and the "streaky" nature of the Stream provide a "real world" situation much more complex than the simple models considered here. Nevertheless, these models do point to basic features that ought to be testable with existing field data or data from future cruises.

Existing data on larval distributions have been taken by: the Soviet vessels "Belegorsk" in March-April, 1979, "Atlant, in Feb-May, 1981, "Evrika", in Feb-Apr, 1982; the Canadian vessels "Gadus Atlantica" in Feb-March, 1981, and 1982, "Lady Hammond" in Feb-Mar, 1982; and the Japanese vessel "K¹ayo Maru" in Jan-Mar, 1982. Most of the data from these cruises have yet to be published, although reports from the 1979 and 1981 cruises, concluded that larvae were most commonly found in Slope Water, but very near to the north wall of the Gulf Stream (Fedulov and Froemam, 1980, Dawe, 1981).

A critical area for a detailed search for spawning Illex illecebrosus is in the Shelf-Slope region southwest of Chesapeake Bay in the December-January period, since this appears from the model to be the most probable area and time to locate the adults, spawn, and larvae. As far as can be determined from the literature, there is almost no existing data on either the presence or absence of squid in this time and space domaine since traditional seasonal surveys in this area have seldom sampled in the Dec-Jan period.

Acknowledgements

The author wishes to acknowledge the members of the Ad Hoc Working Group on Squid Research, of the Northwest Atlantic Fisheries Organization (NAFO) for discussion on a wide range of topics related to the biology and distribution of squid, to K.F. Drinkwater for helpful discussions on the dispersion modelling, to W. M. Petrie for drafting and computational assistance, and to D.L. Allen for typing and editing assistance.

REFERENCES

- Anon, 1981. Provisional Report of the Scientific Council, Northwest Atlantic Fisheries Organization. NAFO SCS Doc. 81/IX/27.

- Beardsley, R.C., W.C. Boicourt, and D.V. Hansen. 1976. Physical Oceanography of the Middle Atlantic Bight. In Middle Atlantic Continental Shelf and the New York Bight. M.G. Gross, ed., American Society of Limnology and Oceanography, Special Symposia, 2, pp 20-34.
- Bigelow, H.B. 1933. Studies of the waters on the Continental Shelf, Cape Cod to Chesapeake Bay. I. The Cycle of Temperature, Pap. Phys. Oceanogr. Meteorol. 2, 1-135.
- Boletzky, S.V., L. Rowe and L. Aroles (1973). Spawning and development of the eggs, in the Laboratory, of Illex coindetii (Mollusca: Cephalopoda). Veliger 15: 257-258.
- Bumpus, D. 1973. A description of the circulation on the Continental Shelf of the east coast of the United States. In Progress in Oceanography, B.A. Warmere, editor. Pergamon Press, 6, 111-157.
- Carter, H.H. and A. Okubo. 1965. A study of the physical processes of movement and dispersion in the Cape Kennedy Area. Chesapeake Bay Institute, Reference 65-2. Report Number NYO-2973-1.
- Ceylone, P.J. and J.L. Chamberlin, 1980. Anticyclonic warm core Gulf Stream eddies off northeastern United States during 1978. Annls. biol., Copenhagen, 35: 50-55.
- Dawe, E.G., P.C. Beck, and H.J. Drew. 1981. Distributions and biological characteristics of young short-finned squid (Illex illecebrosus) in the Northwest Atlantic, February 20-March 11, 1981. NAFO SCR Doc. 81/VI/23.
- Dawe, E.G., P.C. Beck, H.T. Drew and G.H. Winters. 1981. Long-distance migration of a short finned squid (Illex illecebrosus). Northwest Atlantic Fisheries Organization. SCR Doc. 81/VI/24.
- Fedulov, P.P. and Yu. M. Froerman. 1980. Effect of Abiotic Factors on Distribution of Young Shortfin Squids, Illex illecebrosus. NAFO SCR Doc. 80/VI/98.
- Fitzgerald, J. and J.L. Chamberlin. 1980. Anticyclonic Warm Core Gulf Stream Eddies of Northeastern United States during 1979. NAFO SCR Doc. 80/VI/67.
- Fitzgerald, Jayne L. and J. Lockwood Chamberlin. 1981. Anticyclonic Warm Core Gulf Stream Rings off the Northeastern United States during 1980. NAFO SCR Doc. 81/IX/90.

- Iselin, C.O'D. 1936. A study of the circulation of the Western North Atlantic. pap. Phys. Oceanogr. Meteorol. Vol IV, No. 4.
- Kirwan, A.D. Jr., G. McNally and J. Coehlo. 1976. Gulf Stream Kinematics Inferred from a Satellite-tracked Drifter. Jour. Physical Oceanography. Vol. 6. 750-755.
- Lange, A.M. and M.P. Sissenwine. 1981. Evidence of summer spawning of Illex illecebrosus (LeSueur) off the northeastern United States. NAFO SCR Doc. 81/VI/33.
- Mizenko, D. and J. Lockwood Chamberlin. 1979. Anticyclonic Gulf Stream eddies off the northeastern United States during 1976. In Ocean Variability-1976. J.R. Goulet and E.D. Haynes (eds.). NOAA Tech. Rep. N.M.F.S. Circ., 427-259-280.
- O'Dor, R.K., N. Balch, and T. Amaratunga. 1981. The embryonic development of the squid, Illex illecebrosus, in the Laboratory. NAFO SCR Doc. 81/VI/29.
- Okuba, A. and M.J. Karweit. 1969. Diffusion from a continuous source in a uniform shear flow. Limnol. and Oceanogr. 14, 514-520.
- Richardson, P.L. and J.J. Wheat, and D. Bennett. 1979. Free drifting buoy trajectories in the Gulf Stream System (1975-1978). Woods Hole Oceanographic Institution Data Report WHOI-79-4.
- Squires, H.J. 1967. Growth and hypothetical age of the Newfoundland bait squid (Illex illecebrosus illecebrosus). Jour. Fish. Res. Board 24(6): 1209-1217.
- Wiebe, P.H. 1982. Rings of the Gulf Stream. Scientific American, 246(3) 60-70.
- Worthington, L.V. 1954. Three detailed cross-sections of the Gulf Stream, Tellus VI 116-123.
- Wright, W.R. 1976. The limits of shelf water south of Cape Cod, 1941 to 1972. J. Mar. Res., 34(1). 1-14.

TABLE 1

Period when bottom temperature exceeded 13°C, at selected coastal light vessel stations between the Gulf of Maine and Cape Hatteras. Data examined for 1956-60 period.

Lightship	Depth of Observation (m)	Time when Temperature 13°C	Time when Temp. again 13°C	Temp. Max/date
Portland	-	Never reaches 13°		
Boston	29	Rarely reaches 13°		
Georges	17	Early July	Early Nov	18°/Sept.
Nantucket	55	Late Sept	Late Nov.	16°/Oct.
Ambrose	29	Early Aug.	Late Oct.	16°/Sept.
Chesapeake	20	Late May Early June	Late Nov.	21°/Aug.
Diamond	55	Rarely drops below 13° (Occasionally in Jan or Feb)		25°/Oct.

TABLE 2

Form of dispersion parameters for Equation (3) at long times after release of larvae from an instantaneous point source.

Peak Concentration (S_p)	Variance Inflow Direction (σ_x^2)	Variance Normal to flow (σ_y^2)	Stretching Factor, σ_x/σ_y (ρ)
$\frac{3t^{-2}Q}{2\pi A_y \Omega}$	$\frac{2}{3} A_y \Omega^2 t^3$	$2 A_y t$	$\frac{\Omega t}{\sqrt{3}}$

TABLE 3

Patch dispersion characteristics are computed for two geographic positions of the instantaneous point source. A velocity profile as shown in Figure 21 is assumed. In Example 1, the point source is located at the northern edge of the shear zone where the mean velocity is zero at a longitude of 75°W ($\bar{u} = 0, x = 0, y = 0$). In example 2, the point source is located 12 km inside the shear zone where the mean velocity is 72 cms^{-1} ($\bar{u} = 75, x = 0, y = 12 \times 10^5 \text{cm}$).

Time (days)	A_y ($\text{cms}^{-1} \times 10^{-5}$)	Mean Distance Travelled by Patch center (km)	Patch Width, (B) (km)	Patch Length, (L) (km)	$\frac{L}{B}$ ($=\rho$)
Example 1					
5	1	0	12	94	7.8
10	2	0	24	363	15
15	3	0	35	809	23
20	4	0	47	1432	31
30	4	0	58	2615	45
Example 2					
5	1	311	12	176	15
10	2	622	24	704	29
15	3	933	35	1149	33
20	4	1244	47	1771	38
30	4	1866	58	2963	51

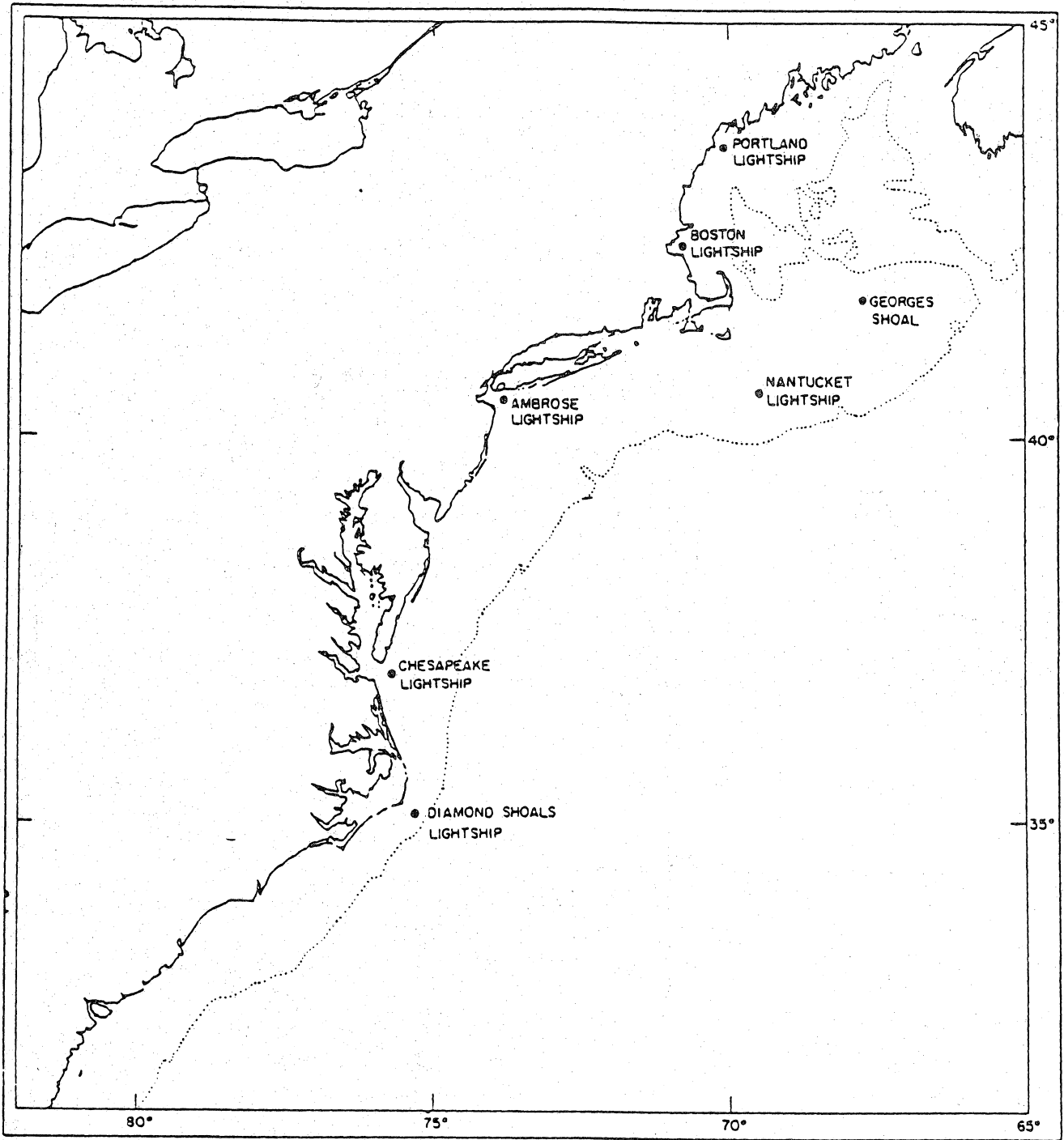


Figure 1 Map showing locations where daily temperature profiles have been taken over a number of years.

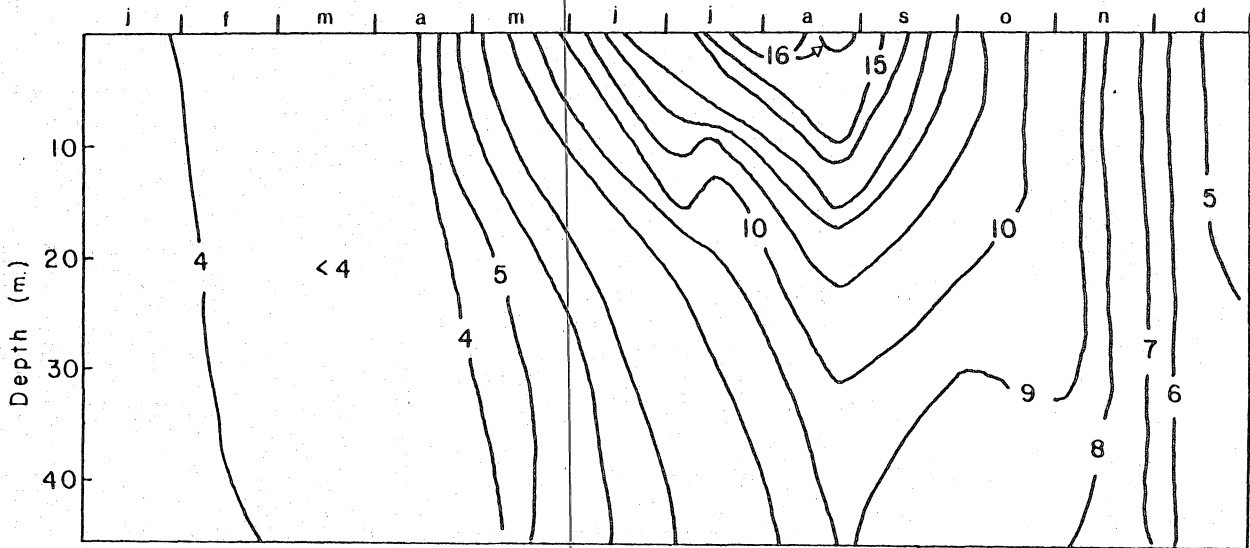


Figure 2 Plot of time-depth temperature structure for Portland Lightship, 1957.

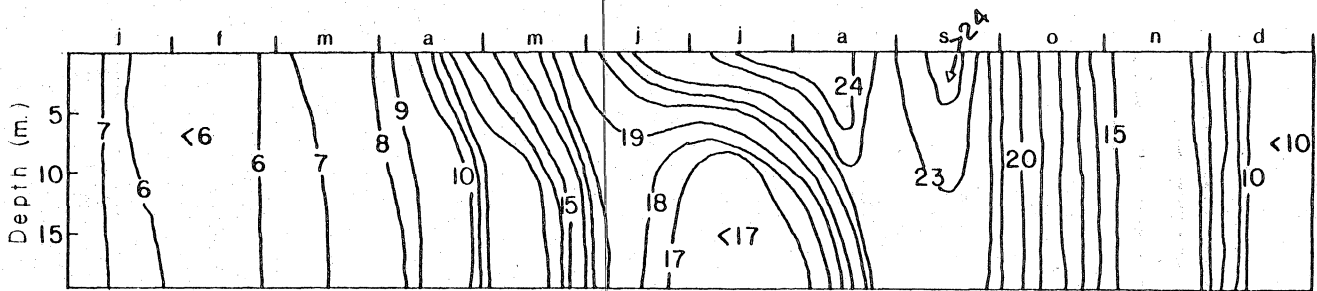


Figure 3 Plot of time-depth temperature structure for Chesapeake Lightship, 1957.

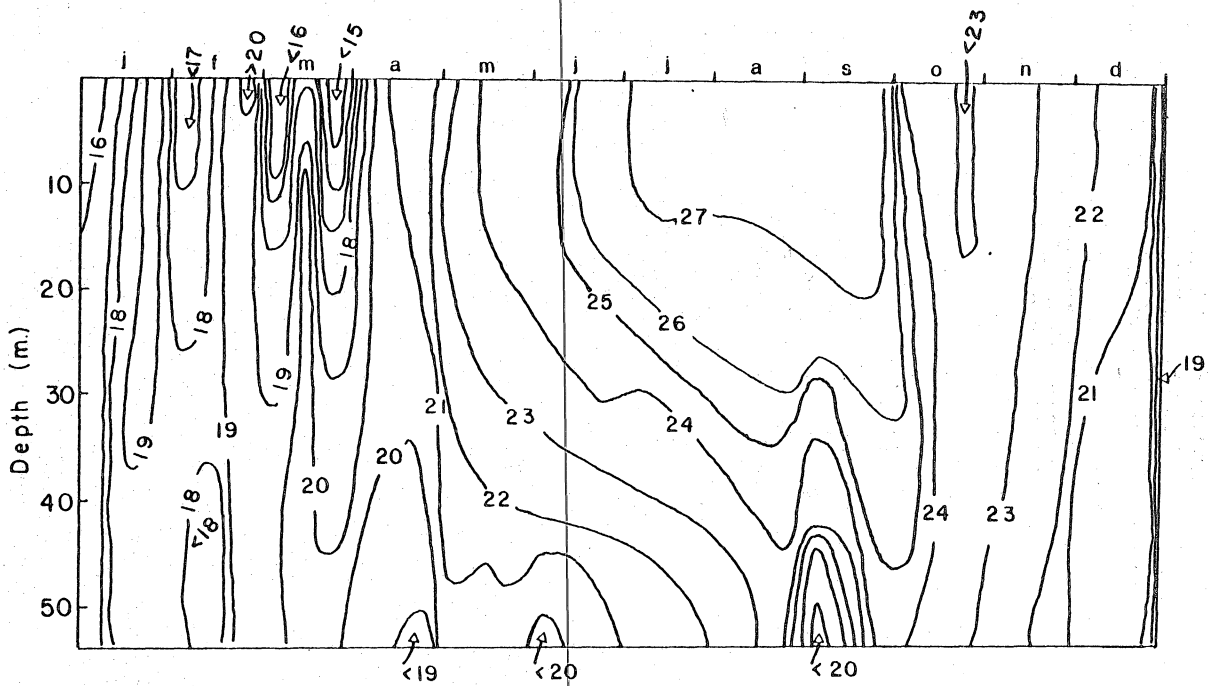


Figure 4 Plot of time-depth temperature structure for Diamond Shoals Lightship, 1957.

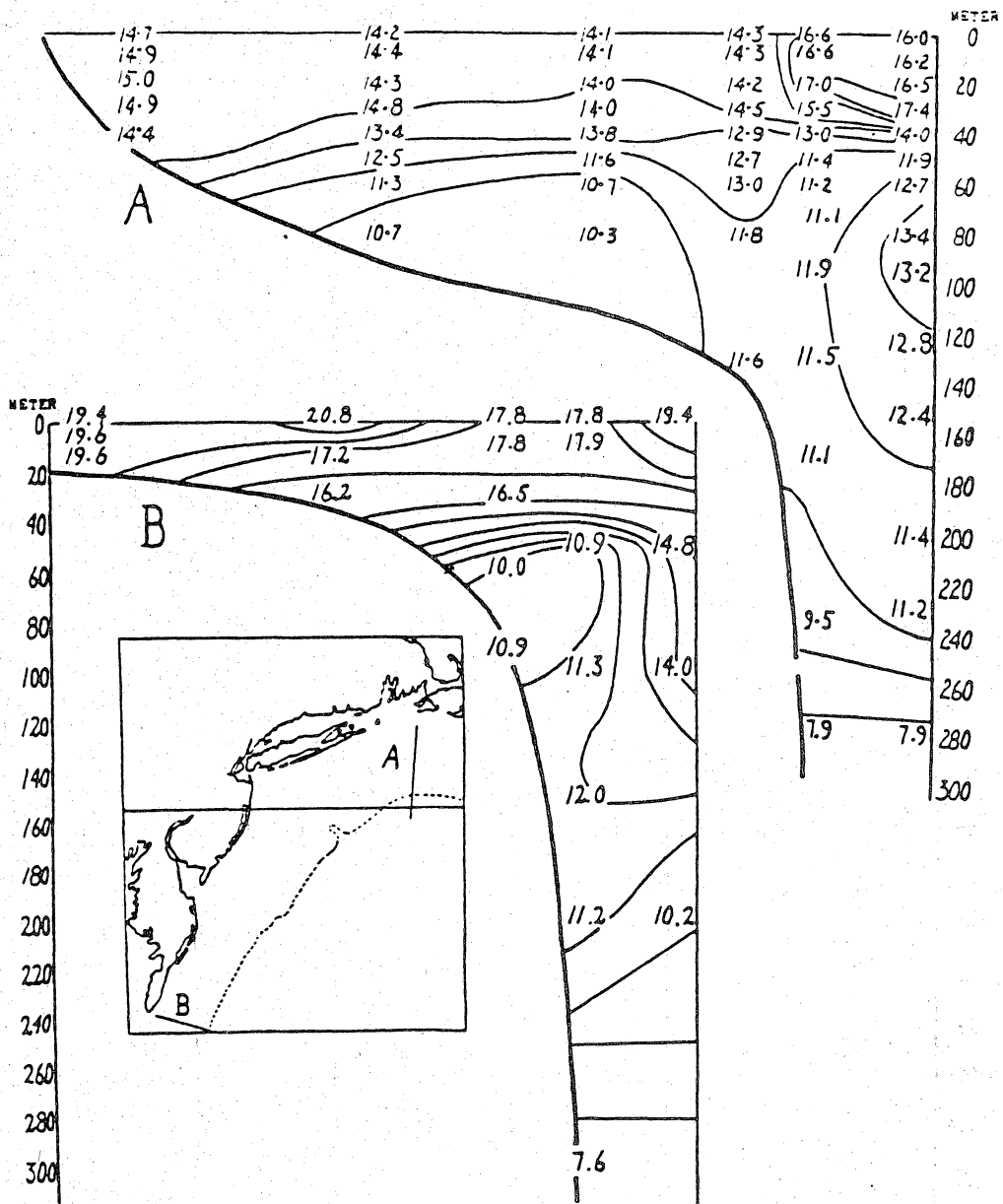


Figure 5 Temperature profiles crossing the Continental Shelf: -A, off Marthas Vineyard, 19 Oct. 1931, and B, off Chesapeake Bay 30-31 Oct., 1919 (from Bigelow 1933).

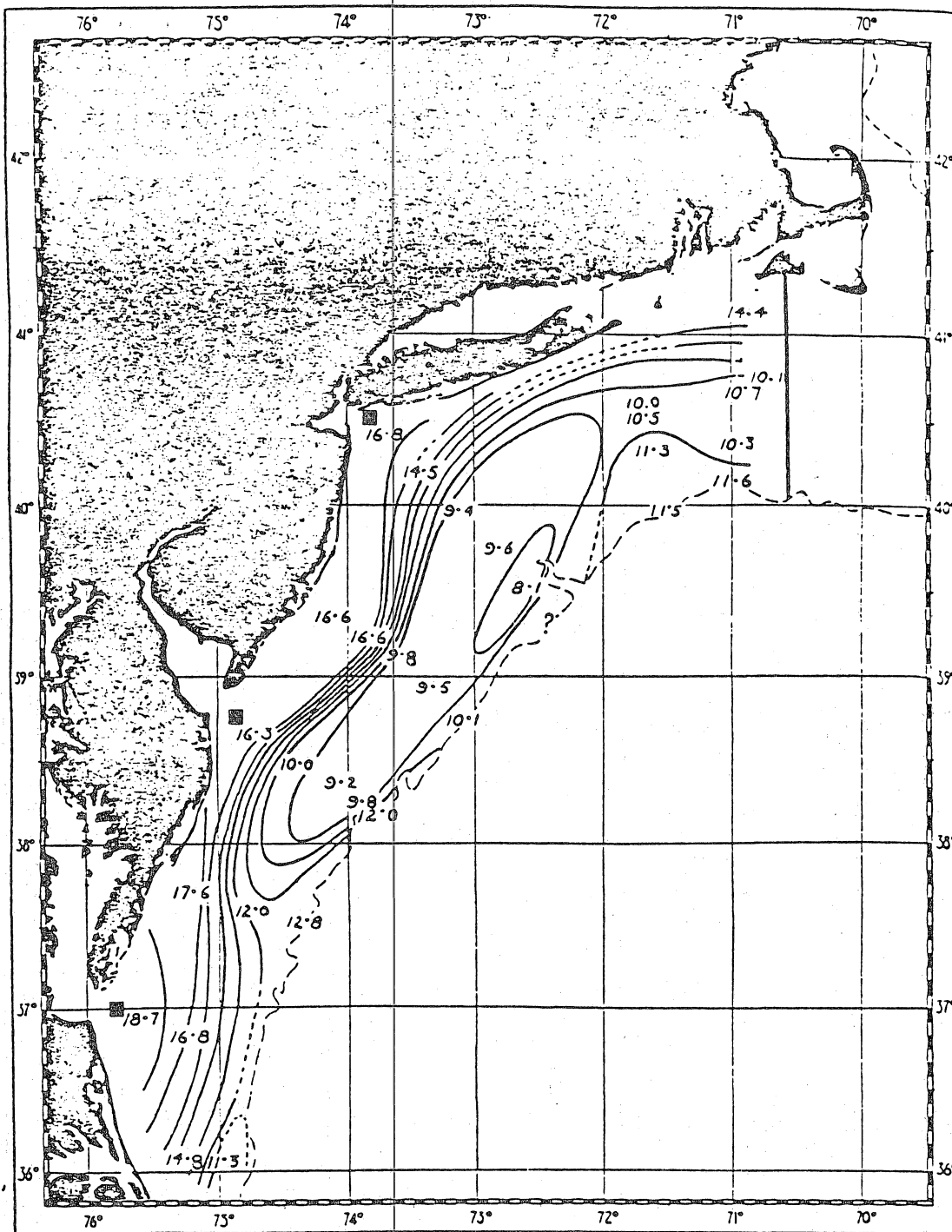


Figure 6 Temperature at the bottom from the 20-metre contour line out to the 150 M depth contour, 19-29 Oct., 1931 (from Bigelow 1933).

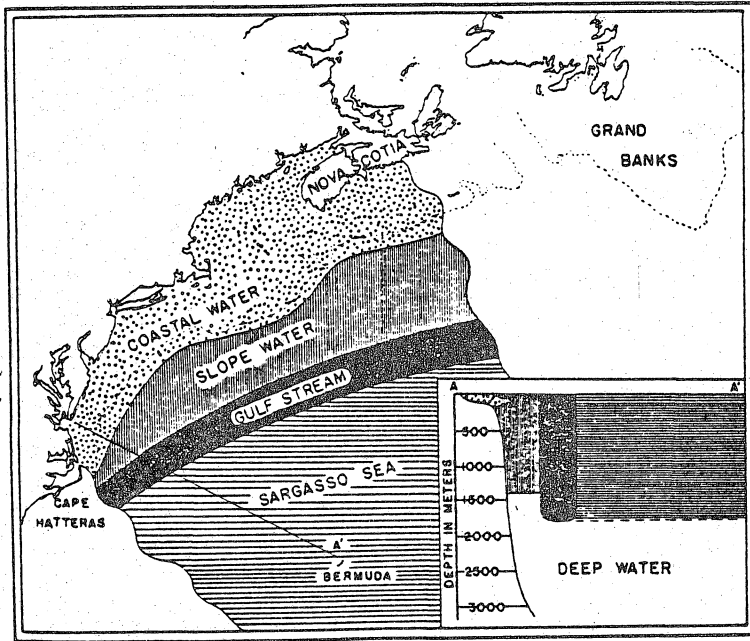


Figure 7 Schematic representation of the water masses in the Nova Scotia-Bermuda-Cape Hatteras triangle (from Iselin, 1936).

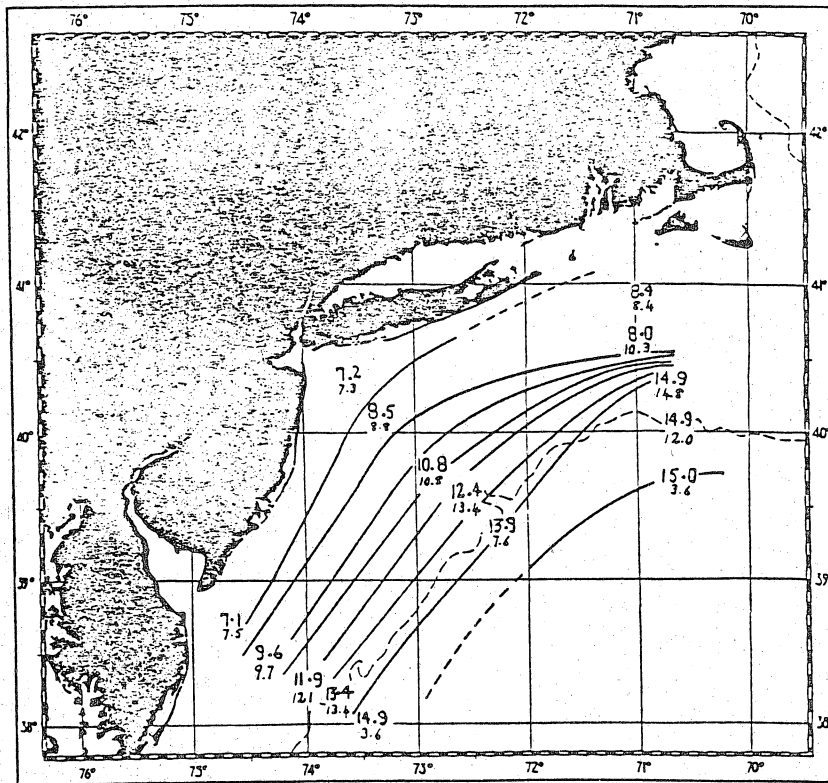


Figure 8 Temperature, 19-21 Dec., 1932. The upper reading of each pair is the surface value and marks the station locality; the lower of each pair is the bottom reading. Isotherms have been contoured for the surface only (from Bigelow, 1933).

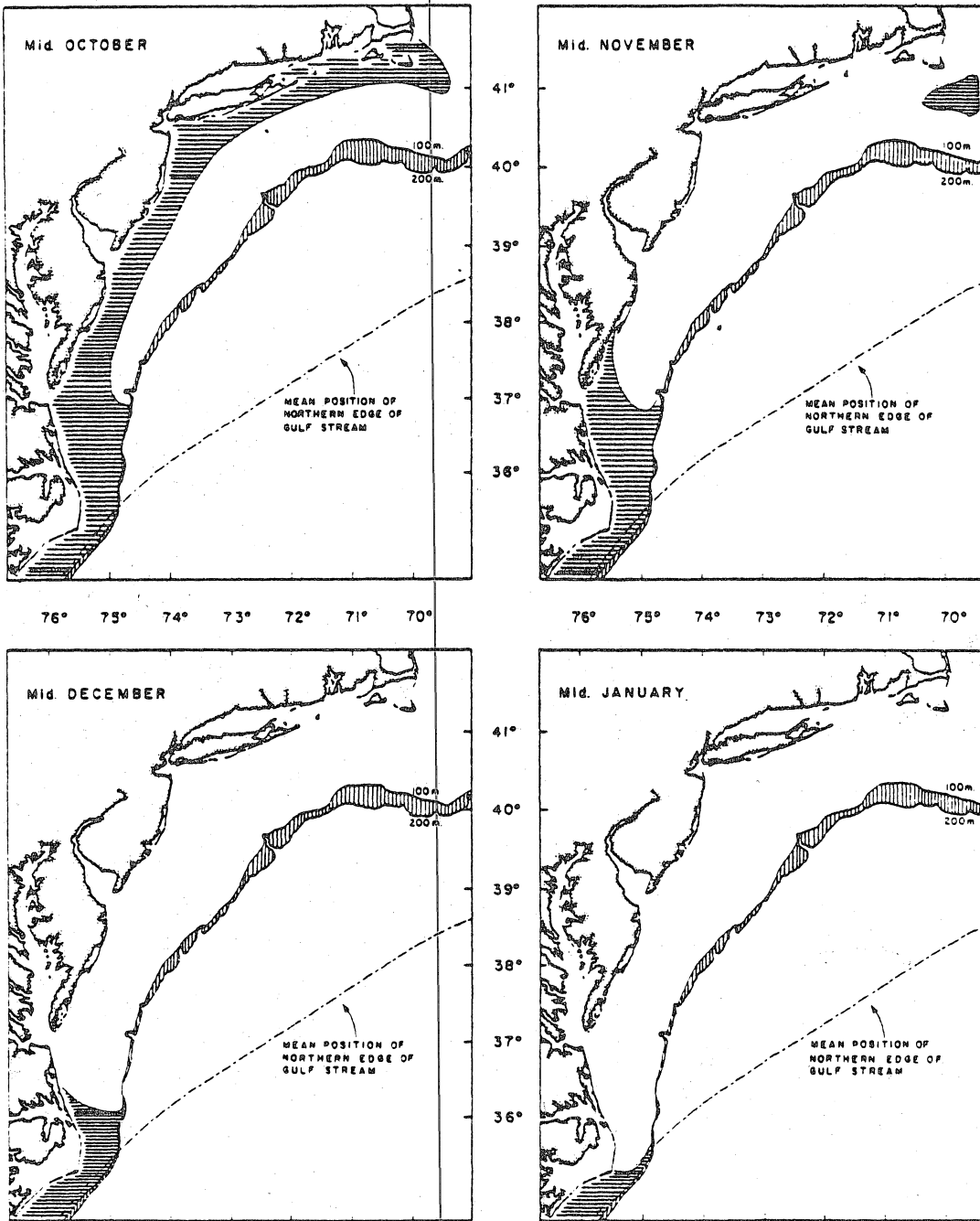


Figure 9 Maps of the Cape Hatteras-Cape Cod region showing the approximate limits where bottom temperatures might be expected to normally exceed 13°C (shaded area) in the mid-October to mid-January period.

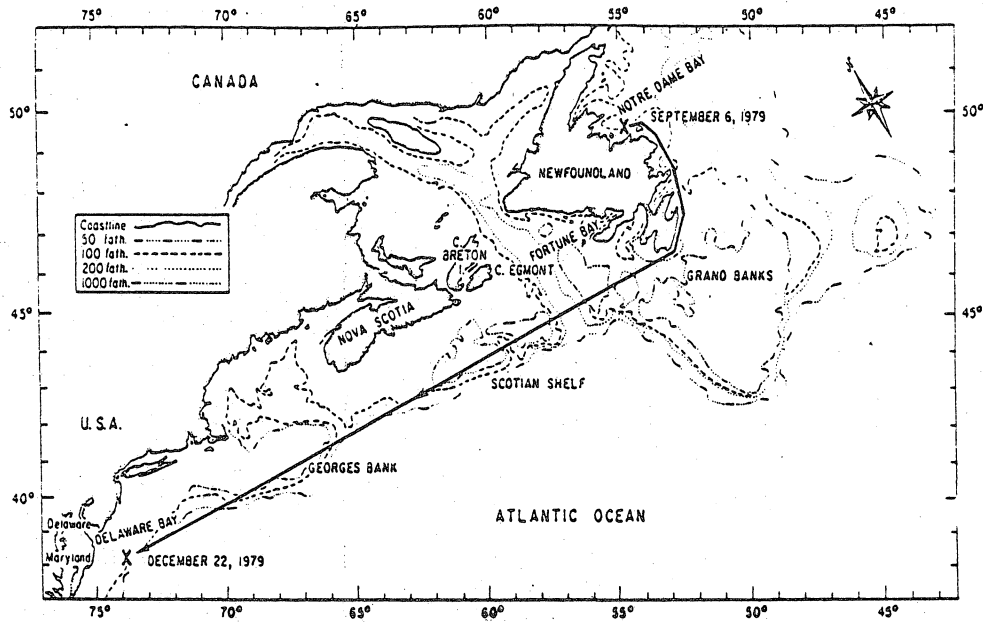


Fig. 10 Map of the northwest Atlantic indicating shortest possible migration route from tagging locality to recapture site (from Dawe et al., 1981).

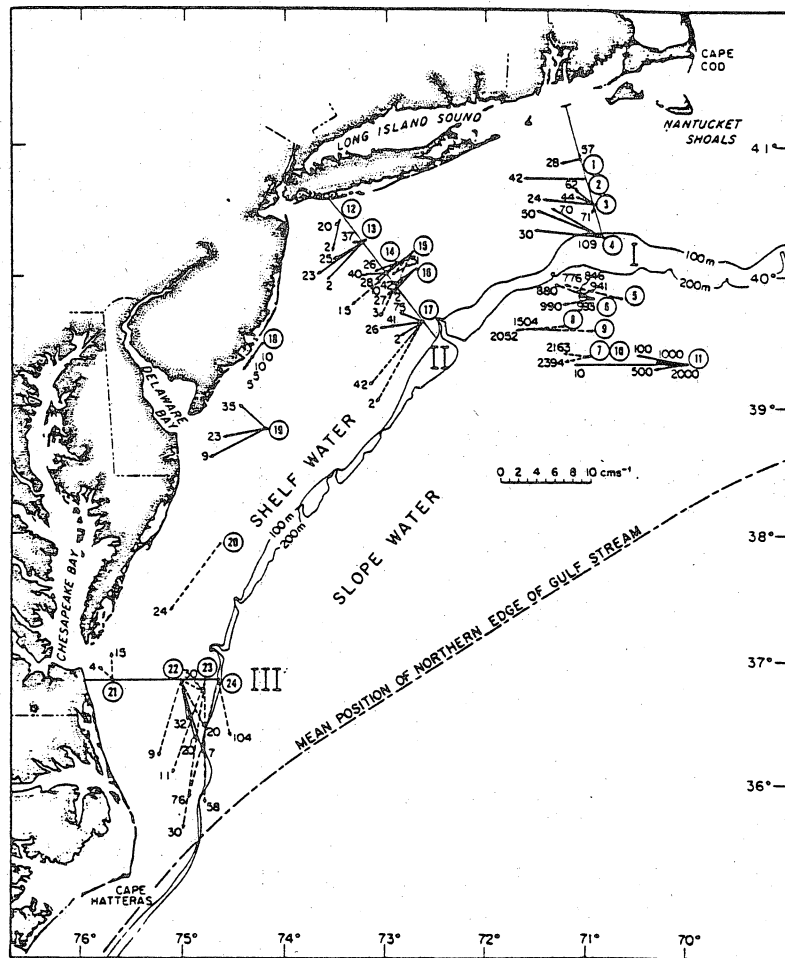


Fig. 11 Mean velocities as measured by moored current meters in the middle Atlantic Bight region. Winter measurements are indicated by solid arrows, while summer velocities are represented by dashed arrows. The individual sites are located at the circles with the station number designated inside the circles. The measurement depths, in metres, are shown near the head of the arrows. (from Beardsley et al., 1976).

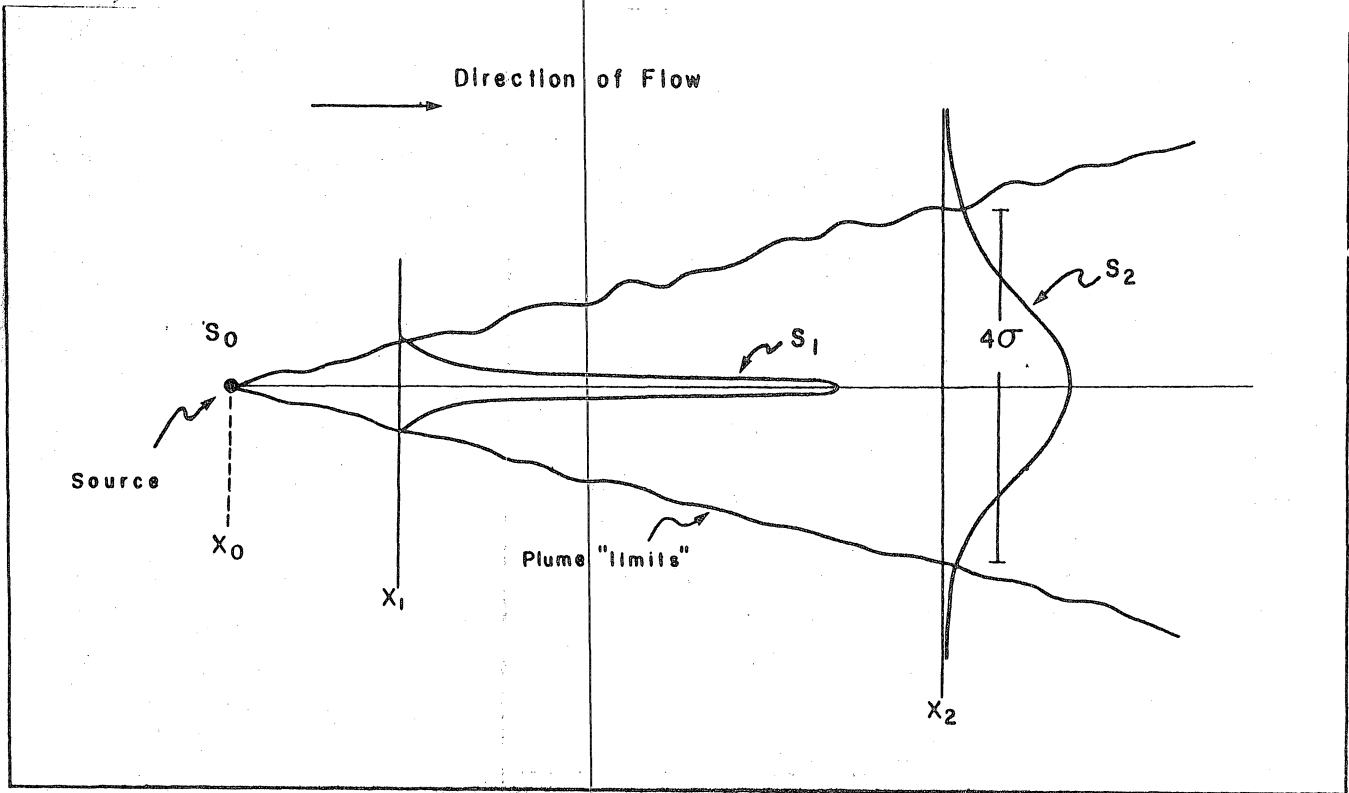


Fig. 12 Schematic illustration of the diffusion of a substance away from a continuous point source in a uniform flow. Typically "Gaussian" profiles of the concentration of the diffusing substance are shown for two cross-sections through the plume downstream from the source. The definition of patch width as four standard deviations (4σ) is designated.

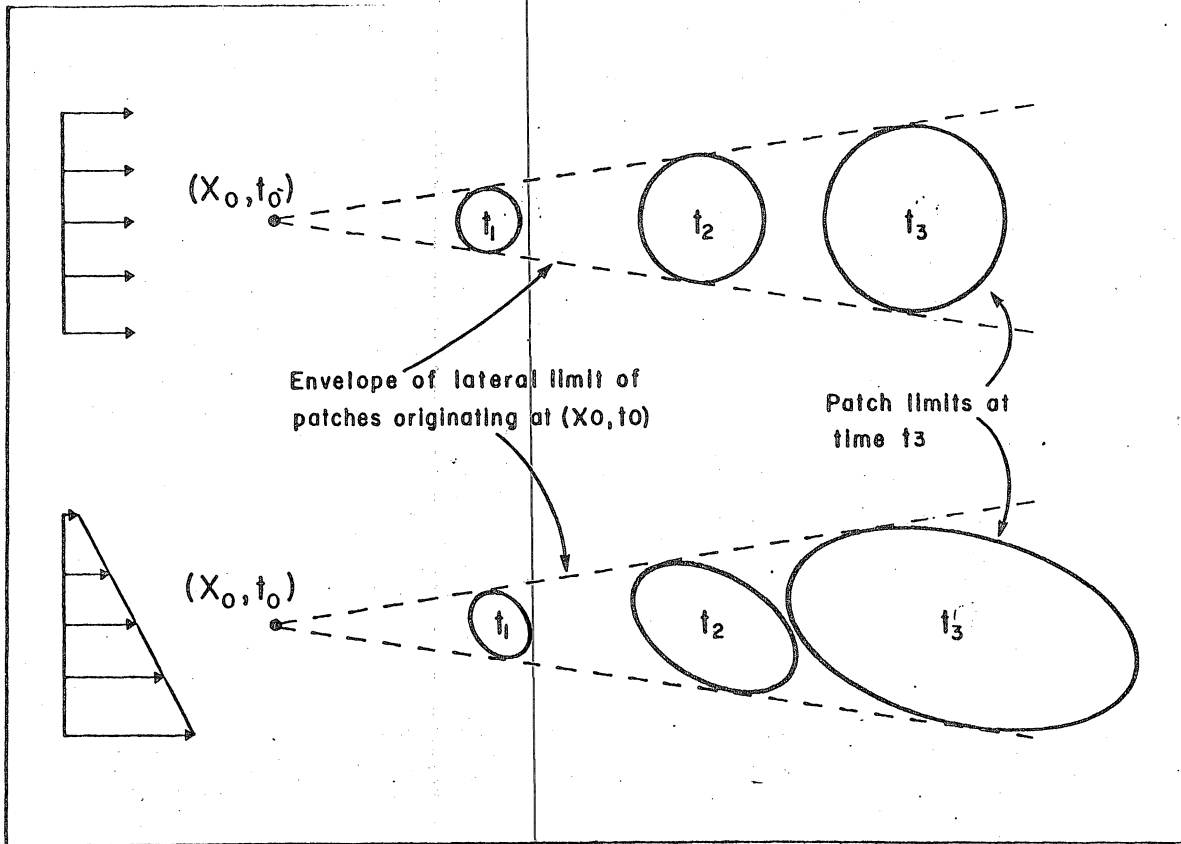


Fig. 13 Schematic illustration of the shape of a patch of diffusing substance in a uniform flow field (upper diagram) and in a shear flow (lower diagram). The patch limits are illustrated for three different times (t_1, t_2, t_3).

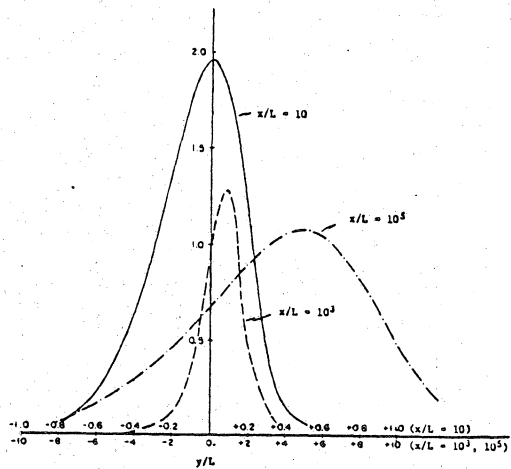


Figure 14 Concentration distribution across a plume in shear flow (from Okubo and Karweit, 1969).

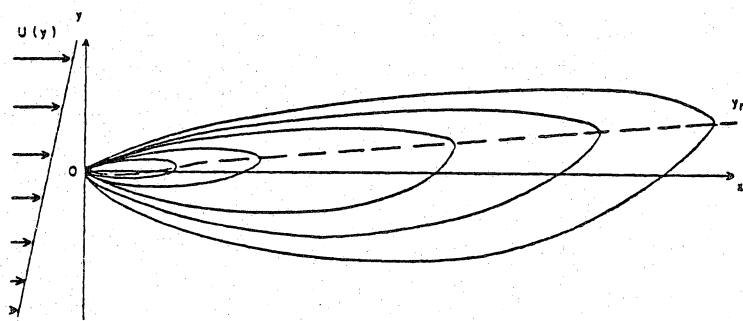


Figure 15 Lines of equal concentration for a continuous plume in shear flow (from Okubo and Karweit, 1969).

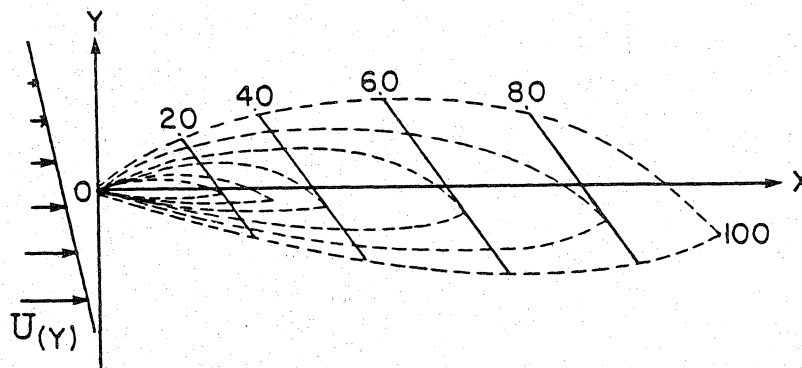


Figure 16 Schematic illustration of the way the larval age-frequency mode may vary geographically. The numbers plotted are merely rough estimates and would vary markedly in actual value depending on the shear, and the diffusion coefficients selected.

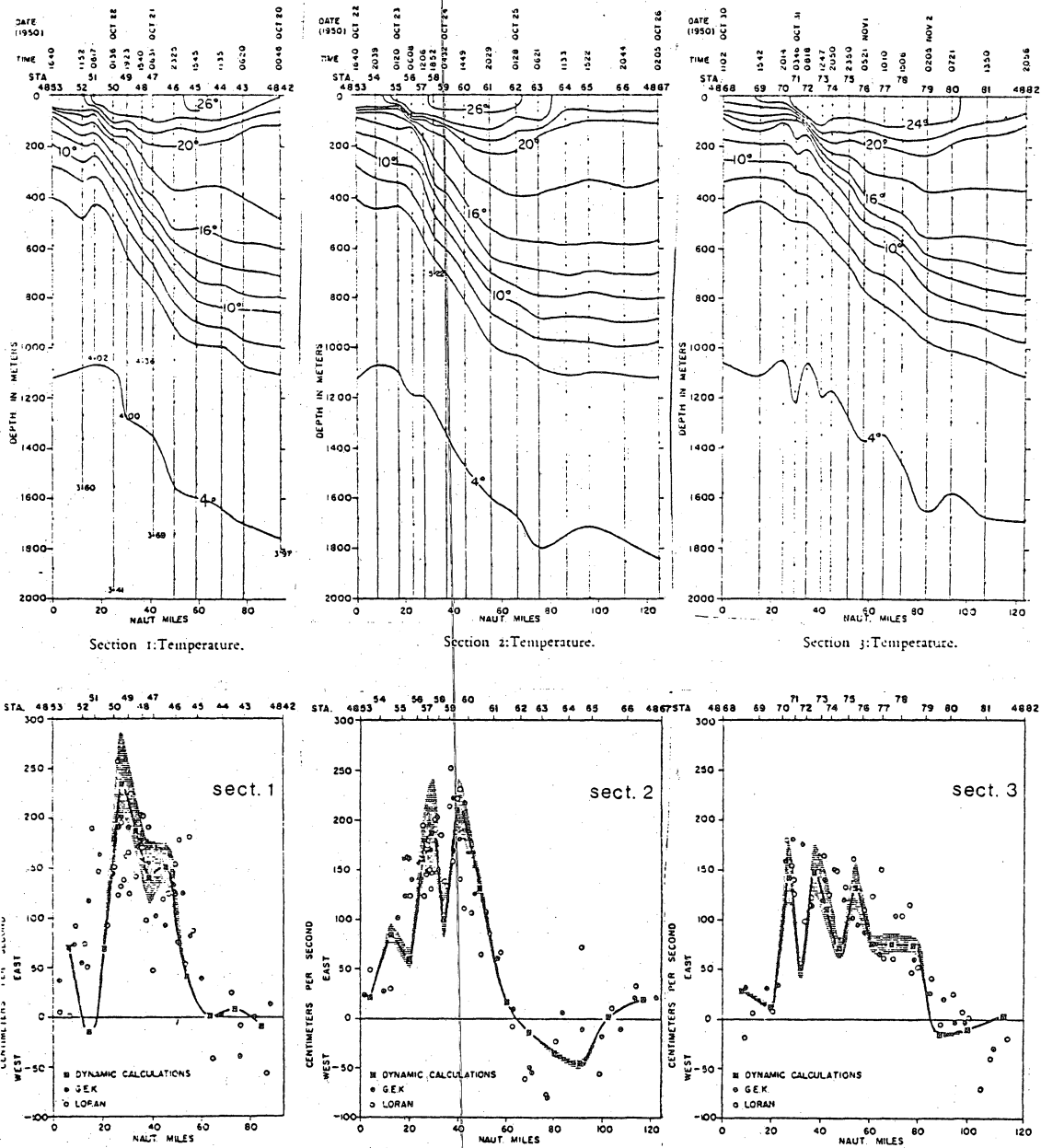


Figure 17 Distribution of temperatures (upper diagrams) for 3 sections across the Gulf Stream in the 68-70°W area for the Oct-Nov 1950 period. Corresponding surface velocities (lower diagram) are shown for GEK, Loran, and from dynamic calculations. (from Worthington, 1954).

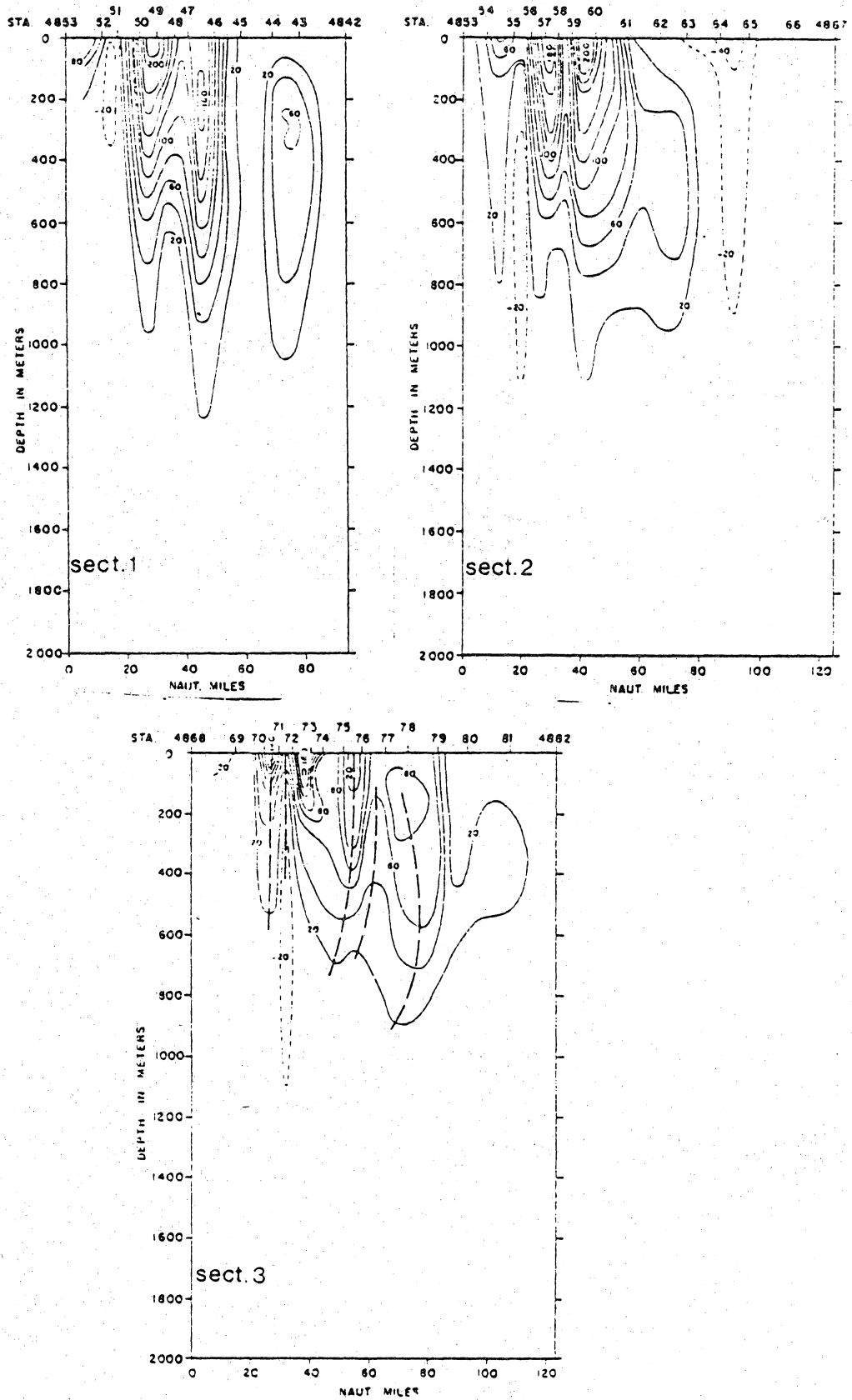


Figure 18 Geostrophic currents in cm S^{-1} are shown for each of the three sections across the Gulf Stream depicted in Figure 17.

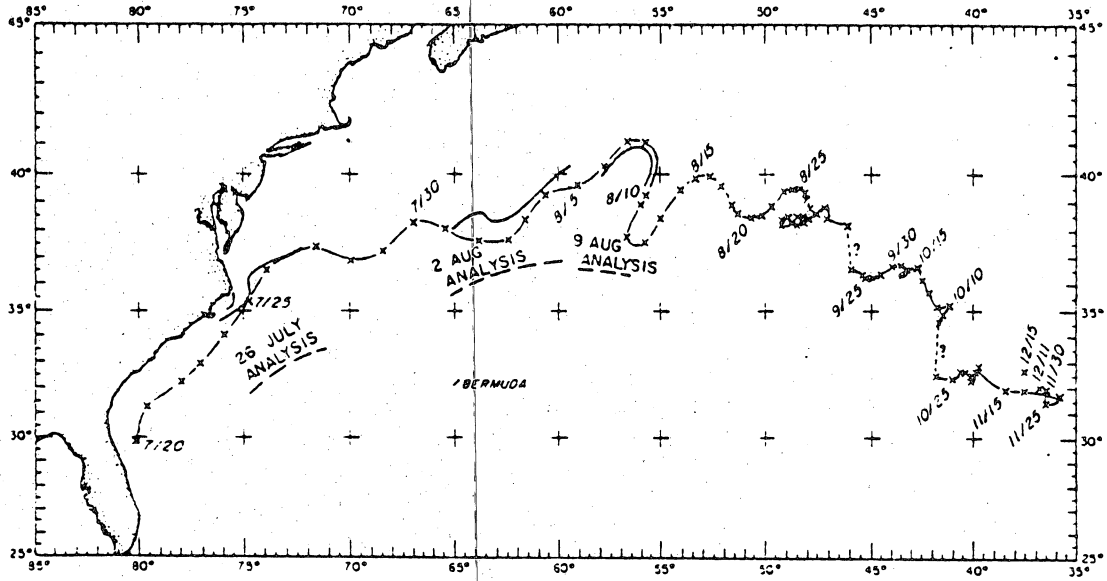


Figure 19 Trajectory for satellite-tracked drifter deployed in the Gulf Stream and tracked for 5 months, in 1975. Buoy was drogued with a parachute and 35 m of cable. (from Kirwan, Jr. et al., 1976).

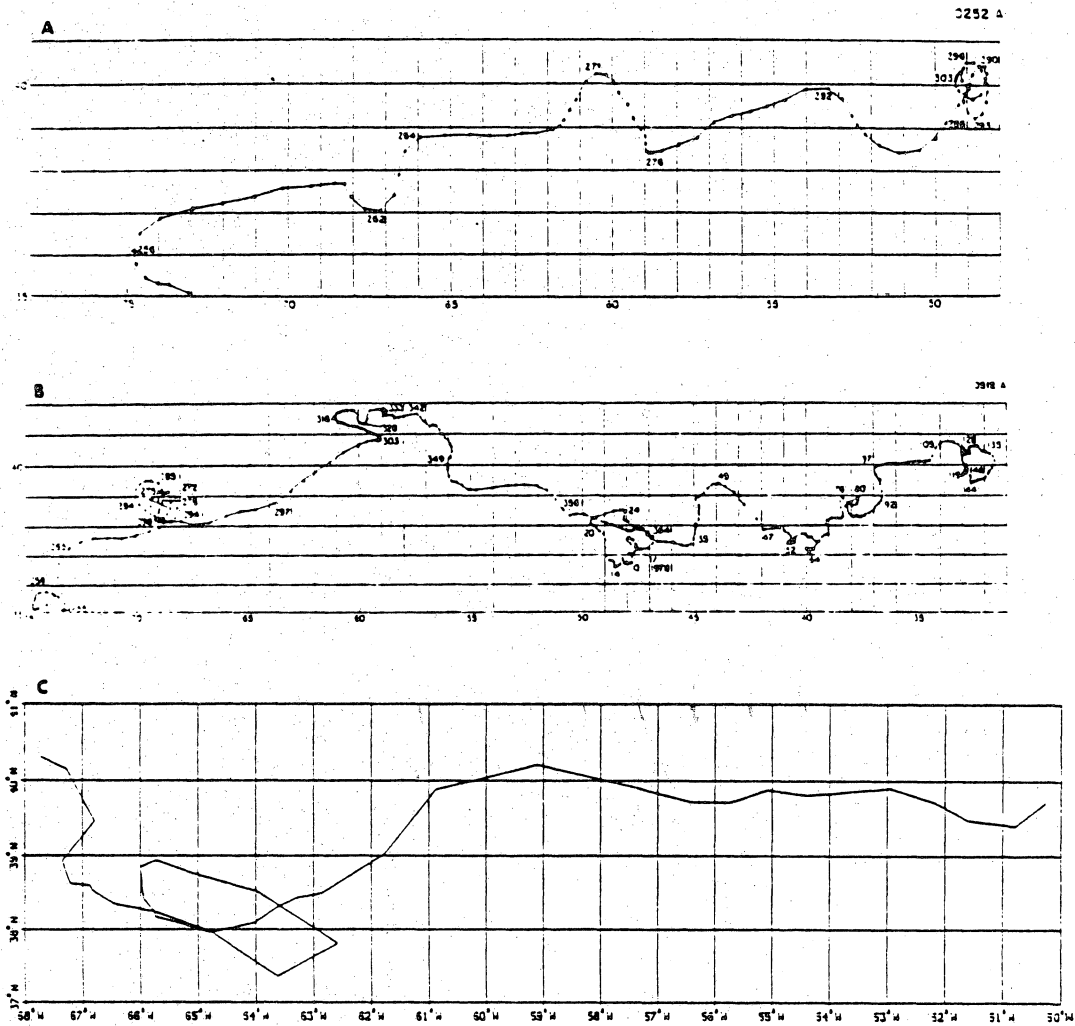


Figure 20 Excerpts from the trajectories of three buoys. A. Trajectory of buoy 0252 from 10 Sept (day 253) to 1 Nov (day 305), 1977. (from Richardson et al., 1979). B. Trajectory of buoy 0512 from 11 Sept (day 254), 1977 to 26 May (day 146) 1978 (from Richardson et al., 1979). C. Trajectory of buoy 1301 released on Browns Bank in October 1979 by the Bedford Institute of Oceanography.

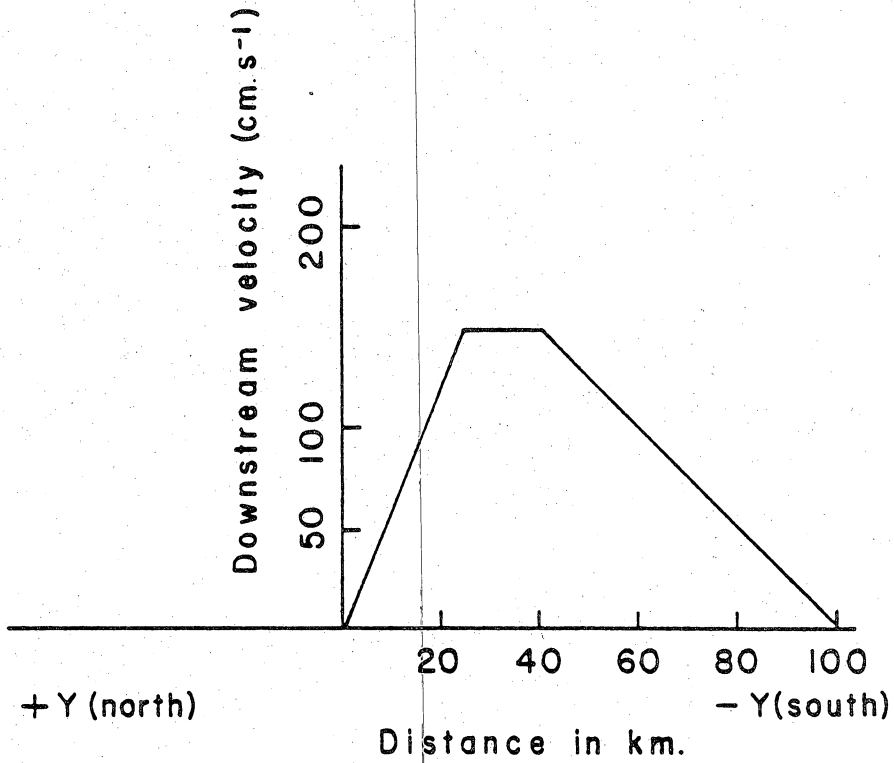


Figure 21 Assumed mean velocity distribution in surface layer across Gulf Stream, between Cape Hatteras and the Tail of the Grand Banks, for use in predicting larval squid patch size and location.

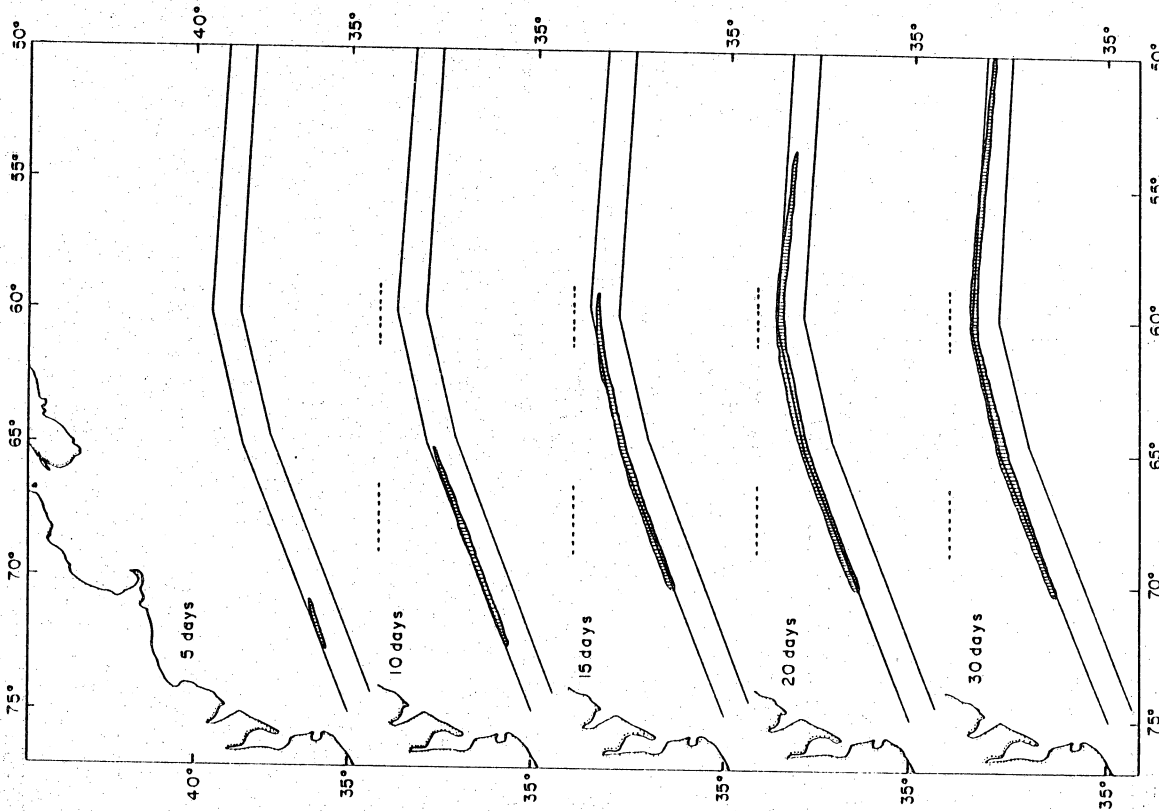


Figure 22: Plots of patch location and size for a point source release at edge of the shear zone (Example 1, Table 3) at end of 5, 10, 15, 10, and 30 days.

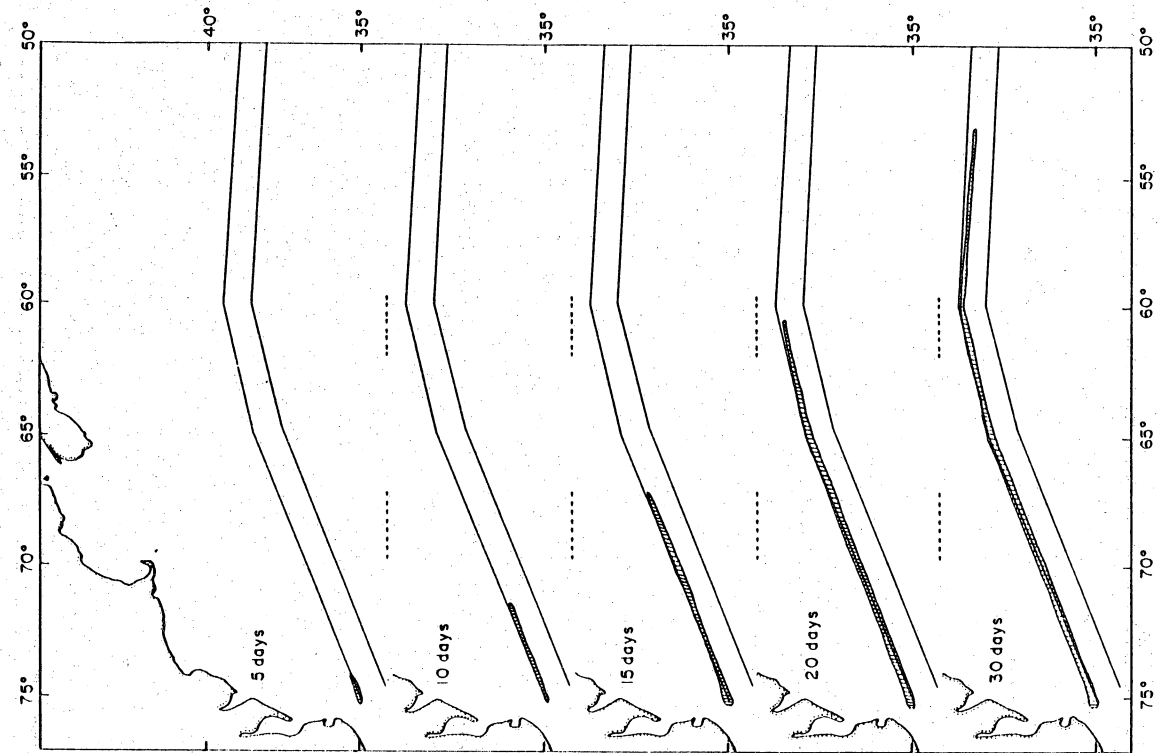


Figure 23: Plots of patch location and size for a point source release 12 km inside shear zone (Example 2, Table 3) at end of 5, 10, 15, 10, and 30 days.

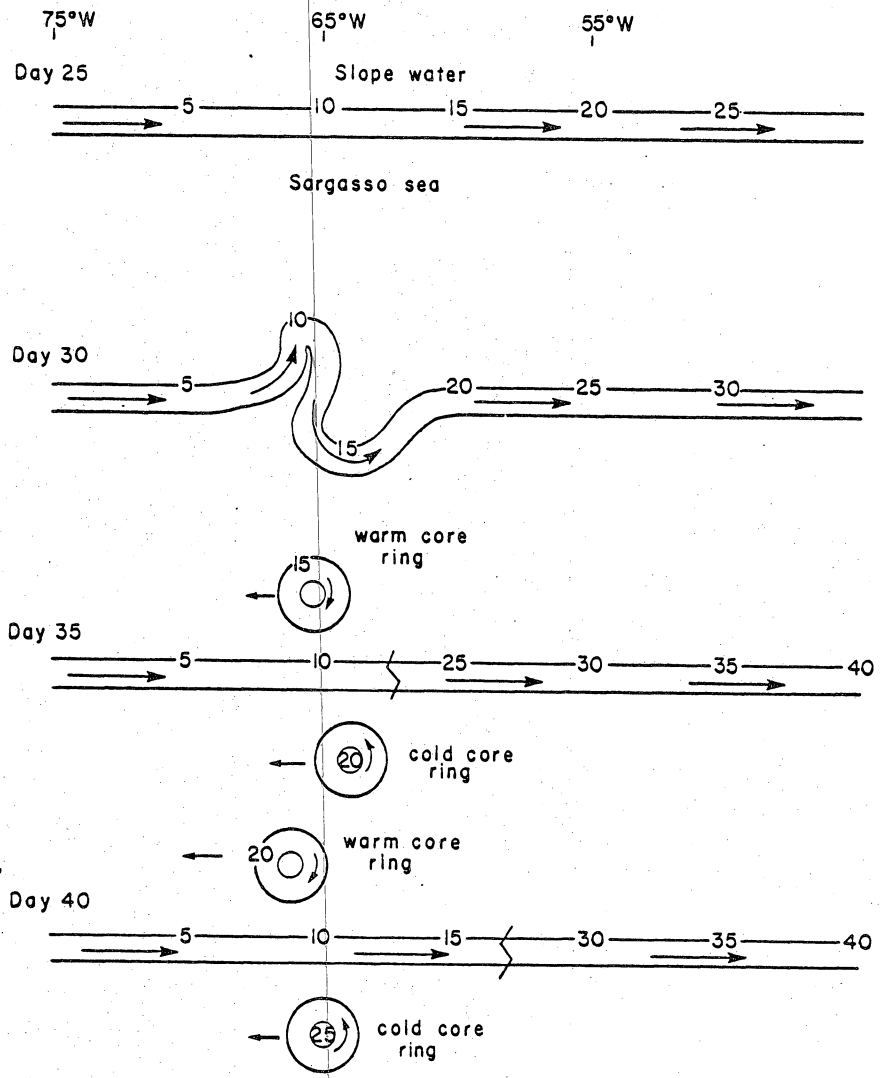


Figure 24 Schematic illustration of the resulting larval patch ensemble distribution during and following the formation of Gulf Stream eddies.